

MIMO Channel Sounder at 3.5 GHz: Application to WiMAX System

H. Farhat, G. Grunfelder, A. Carcelen and G. El Zein
Institute of Electronics and Telecommunications of Rennes (IETR/UMR CNRS 6164)
INSA – 20 Av. des Buttes de Coësmes, CS14315, 35043 Rennes Cedex, FRANCE
Email: hanna.farhat@insa-rennes.fr

Abstract—The use of antenna arrays at emission and reception seems to represent a prominent solution for future wireless systems, it improves data rates and enhances the quality of service. The performance of these systems depends mainly on the propagation channel. Therefore, channel's characterization and modeling are crucial. In this document, we present a MIMO (Multiple Input Multiple Output) channel sounder at 3.5 GHz developed at IETR. One of the applications operating at this frequency is the WiMAX system. Different antenna arrays architectures are designed and calibrated at 3.5 GHz for high resolution MIMO channel sounding. Antenna arrays beam patterns are measured and calibrated. The importance of this work is shown by ESPRIT simulations. Propagation measurement results are needed to obtain realistic MIMO channel models.

Index Terms—Antenna arrays, radio propagation, wireless channel characterization and modeling, spatio-temporal measurements, MIMO channel sounder.

I. INTRODUCTION

In order to deal with needs in terms of number of users and high data rates, due to the development of the multimedia services in wireless systems, the MIMO concept is an attractive solution in the development of the forthcoming generation of broadband wireless networks.

By simultaneously using multiple antennas at both emission and reception sites, these systems exploit the spatial dimension of the propagation channel. This particular configuration allows the system's capacity to increase in the presence of multi-path propagation [1] [2]. Consequently, the MIMO technology was adopted in the new standards IEEE 802.11n (future WiFi) and IEEE 802.16e (future WiMAX).

The expected performances of MIMO systems depend on the spatio-temporal characteristics of the propagation channel that must be accurately specified. In particular, the directional properties should be known at both communication link sides. A MIMO channel sounder was developed at IETR laboratory at 2.2 GHz frequency [3], and was also extended to the 3.5 GHz. This frequency bandwidth concerns WLL (Wireless Local Loop) applications like the WiMAX system.

Our research shows that there are some published results of double directional channel measurements, however not for similar frequencies. These measurements are needed to obtain realistic MIMO channel models for new wireless systems design and simulation.

To improve propagation parameters estimation, like the Direction of Arrival (DoA) and the Direction of Departure (DoD), high resolution algorithm unitary ESPRIT (Estimation of Signal Parameters via Rotational Invariance Techniques) [4] is used with planar arrays architectures [5] like ULA (Uniform Linear Array) and URA (Uniform Rectangular Array). This algorithm is very sensitive to antenna array imperfections, since it relies on identical beam patterns. In fact, any beam pattern ripple can be interpreted as phantom wave front. That reduces the measurement's dynamic range, accuracy, and may lead to wrong estimates. Consequently, calibration procedure is needed. This work was presented in [6]. New antenna arrays were also designed and will be presented later.

The structure of this paper is as follows. In section II, the double directional propagation channel is presented. In section III, the developed MIMO channel sounder is discussed. In section IV, an overview of the designed antenna arrays, and the effects of imperfections on the arrays beam patterns is highlighted. In section V, a calibration algorithm is applied on measured beam patterns and the calibration results are presented. In section VI, simulation results with unitary ESPRIT algorithm are included, in order to show the importance of the calibration procedure. Also, new antenna arrays architecture are described in section VII. Finally, section VIII concludes the paper and draws some perspectives of this work.

II. DOUBLE DIRECTIONAL RADIO CHANNEL

The double directional radio propagation channel was defined in [7]. The corresponding impulse response includes all L resolvable propagation paths between the position r_{Tx} of the transmitter (Tx) and the position r_{Rx} of the receiver (Rx). This model considers ideal omnidirectional antennas [8], and all parameters to be constant in time. The time invariant channel impulse response is defined by:

Part of this work was presented at IEEE Vehicular Technology Conference (VTC Fall 2007) Baltimore, USA.

$$h(r_{Tx}, r_{Rx}, \tau, \phi, \theta) = \sum_{l=1}^L h_l(r_{Tx}, r_{Rx}, \tau, \phi, \theta) \quad (1)$$

where τ is the excess delay, ϕ the DoD (Direction of Departure), and θ the DoA (Direction of Arrival). For planar waves the contribution of the l_{th} propagation path is:

$$h_l(r_{Tx}, r_{Rx}, \tau, \phi, \theta) = a_l \delta(\tau - \tau_l) \delta(\phi - \phi_l) \delta(\theta - \theta_l) \quad (2)$$

where a_l is the complex amplitude, τ_l the excess delay, ϕ_l the DoD, and θ_l the DoA corresponding to the l_{th} path. The main objective of our work is to measure this double directional channel impulse response and to determine the propagation paths parameters. The gathered information should lead to realistic MIMO channel models.

III. MIMO CHANNEL SOUNDER

The performance of MIMO systems depends on the double directional propagation channel properties. That is why a variety of MIMO channel sounders were developed [9]-[11] in order to characterize propagation path parameters like DoA, DoD, in addition to delay, Doppler, polarization and path loss. The majority of measurement results presented with these channel sounders are in the 5 GHz band. Furthermore, a wideband MIMO channel sounder (Fig. 1) was developed in our laboratory. Initially, it operated at 2.2 GHz RF (Radio Frequency) for UMTS and WLAN applications and was then extended to 3.5 GHz RF. The sounder uses a periodic PN coded transmit signal based on the spread spectrum technique. This sounder offers a temporal resolution about 11.9 ns with 100 MHz sounding bandwidth. The loss of about 20% in the theoretic temporal resolution (10 ns) is due to the filtering effect.

Other sounding bandwidths can be used like 50, 25 and 12.5 MHz in environments where the temporal resolution can be reduced. Different impulse response lengths can be recorded from 1.27 to 81.84 μ s, depending on the sounding bandwidth and the chosen code length. As an example, with 100 MHz sounding bandwidth and 1023 code length, the impulse response is recorded for 10.23 μ s. The best dynamics obtained on the channel impulse response is 50 dB for the 1023 PN code length.

The LO (Local Oscillator) units generate carrier waves at 2.45 and 3.75 GHz and then mixed with IF = 250 MHz (Intermediate Frequency) signal and band-pass filtered to obtain the two desired sounding frequency bands. The synchronization between the transmitter and the receiver is achieved with highly stable 10 MHz rubidium oscillators. A system calibration is performed; we connect the Tx RF output to the Rx RF input through appropriate variable attenuators and the calibration is

applied for all AGC (Automatic Gain Control) values with a 5 dB step. After the development of the transmitter and receiver parts of the channel sounder, multiple antenna arrays architecture are also designed in the two frequency bands. In this paper, we only describe the antenna arrays at 3.5 GHz.



Figure 1. MIMO channel sounder transmitter and receiver.

IV. ANTENNA ARRAYS DESIGN

Two ULA antennas for transmission and reception are designed at 3.5 GHz for double directional channel sounding in outdoor environments and for fixed measurements configuration.

The antenna array single element is simulated with the HFSS tool and implemented in our laboratory. The objective was to obtain a bandwidth of 200 MHz at the center frequency of 3.5 GHz. Fig. 2 presents the simulated and measured return loss of the single element. In spite of the difference between simulation and measurement, the obtained result shows that the antenna matched well to the desired application. The average gain of the single antenna element is 7 dB.

The transmitter array (Tx) contains 4 active elements and 2 passive edge elements to reduce the influence of environmental reflections, and also to avoid any pattern discontinuity (Fig. 3). We integrate power amplifiers near antennas to increase transmitted power.

Fig. 4(a) shows the antennas measured beam patterns, with electronic components (switch, power amplifiers, phase shifters, and so forth), of the 4-element ULA Tx at 3.5 GHz. We can notice that the difference between the 4 plots magnitudes is minimal. Fig. 4(b) shows the beam patterns ripple at 3.5 GHz of the 4-element ULA Tx array. It is caused by impairments like length difference between feeder cables, geometrical and electrical tolerances in addition to mutual coupling between elements. The ripple value varies from -1.3 to 0.9 dB.

The receiver array (Rx) contains 8 active elements and 2 passive edge elements (Fig. 5). We integrate LNAs

(Low Noise Amplifiers) to have a good measurement dynamic. This integration of LNAs following antennas permits us to reduce the noise figure of the receiver to 4 dB. Fig. 6(a) shows the antennas measured beam patterns with electronic components of the 8-element ULA Rx at 3.5 GHz. The observed difference between the 8 plots (about 3 dB) is due to the 8 LNAs gain difference. Fig. 6(b) shows the beam pattern ripple at 3.5 GHz for the 8-element ULA array. The ripple value varies from -0.9 to 0.9 dB. The calibration of the measured beam patterns is necessary for the Tx and Rx arrays to reduce ripple values.

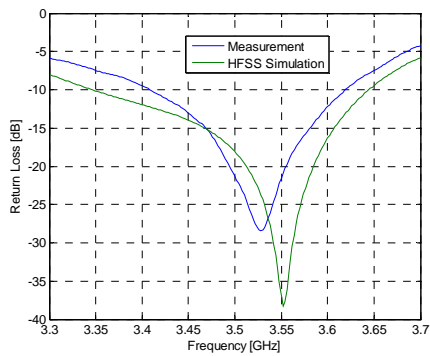


Figure 2. Single element antenna return loss.

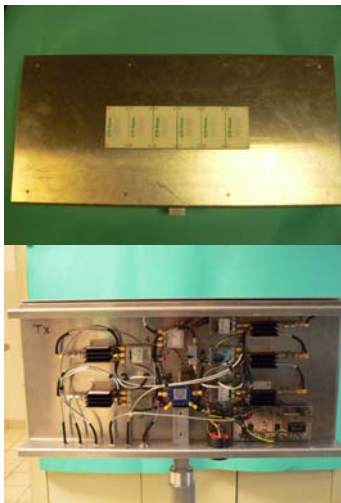


Figure 3. Four elements ULA array transmitter.

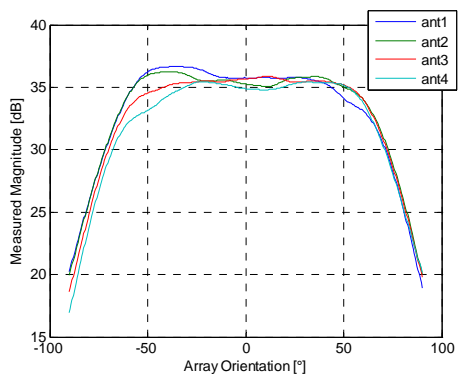


Figure 4(a). Measured beam patterns of 4 elements ULA Tx.

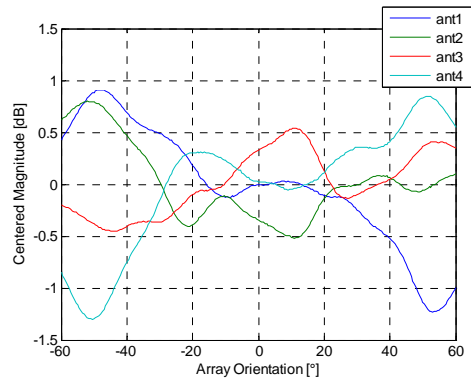


Figure 4(b). ULA Tx beam patterns ripple.



Figure 5. Eight elements ULA array receiver.

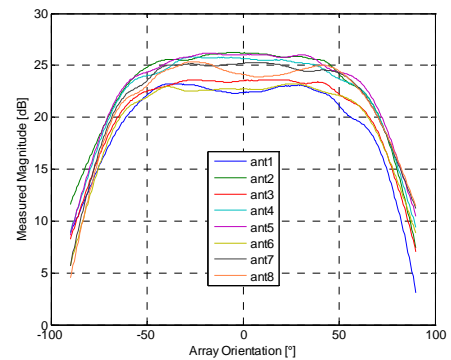


Figure 6(a). Measured beam patterns of 8 elements ULA Rx.

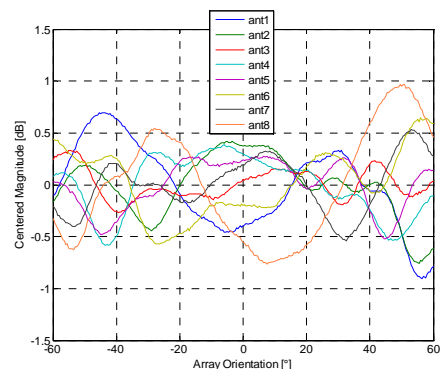


Figure 6(b). Eight elements ULA Rx beam patterns ripple.

V. ANTENNA ARRAYS CALIBRATION

The calibration procedure is based on N reference measurements in anechoic chamber. A reference antenna is placed on an equidistant grid of known azimuth angles. Zero degree azimuth angle is defined in the perpendicular plan to the array (broadside direction). For more convenience, the reference antenna is kept fixed and the array is being rotated around its phase center. The distance between the Tx and the Rx antennas is 9.5 m which is higher than 100λ at 3.5 GHz. This distance is required to get plane wave fronts at the antenna array [12], thus the far field condition is fulfilled.

The used calibration algorithm was presented in [13], and adopted for antenna array calibration in [12].

The performance of this calibration algorithm has been demonstrated in [14].

In the ULA geometry case (M elements spaced by d), in ideal case, if a single planar wave front with complex attenuation γ , from the azimuthal direction θ_v impinges. The array response vector results in

$$\mathbf{x} = \mathbf{a} \gamma \quad (3)$$

where \mathbf{a} is the array steering vector given by

$$\mathbf{a}(\theta_v) = \begin{bmatrix} 1 & e^{-j2\pi\frac{d}{\lambda}\sin\theta_v} & \dots & e^{-j2\pi(M-1)\frac{d}{\lambda}\sin\theta_v} \end{bmatrix}^T \quad (4)$$

In the real case, the measured array response vector becomes

$$\mathbf{x}_m = \mathbf{K}\mathbf{a}\gamma + \mathbf{n} \quad (5)$$

where \mathbf{n} is the additive noise and \mathbf{K} ($M \times M$) is the error matrix that describes the array imperfections.

The main diagonal of \mathbf{K} matrix contains the amplitude and phase errors of the antennas and electronic components. The calibration algorithm calculates the correction matrix $\mathbf{K}_{cal} = \mathbf{K}^{-1}$ that removes the systematic error if applied to the array output.

The proposed algorithm to estimate \mathbf{K}_{cal} is based on the idea that for an error-free array, a set of orthogonal null steering vectors $\mathbf{c}_\mu(\theta_v) = \mathbf{a}(\theta_v)e^{-j2\pi\mu/M}$ exists where $1 \leq \mu \leq M-1$.

Fig. 7(a) presents the calibrated beam patterns obtained at 3.5 GHz after the application of the calibration algorithm for the ULA Tx, and Fig. 7(b) the beam patterns ripple. We can notice that the ripple between the 4 plots is significantly reduced to ± 0.5 dB.

Fig. 8(a) presents the calibrated beam patterns obtained at 3.5 GHz for the ULA Rx, and Fig. 8(b) the beam patterns ripple. We can notice that the ripple between the 8 plots is significantly reduced below ± 0.5 dB. Fig. 9(a) and (b) show the measured phase of ULA Rx before and after calibration. We can observe the correction effect especially in the broadside direction.

A. Edge elements importance

We study the edge elements influence on the beam patterns ripple, namely for the Tx array. We added two

additional edge elements, and the beam patterns were measured again in anechoic chamber. Fig. 10 shows the two measured configuration with 2 and 4 edge elements. Fig. 11 (a) and Fig. 11 (b) present the beam patterns ripple for the 4-element ULA Tx before and after calibration. We can observe more reduction of the ripple values with this new configuration.

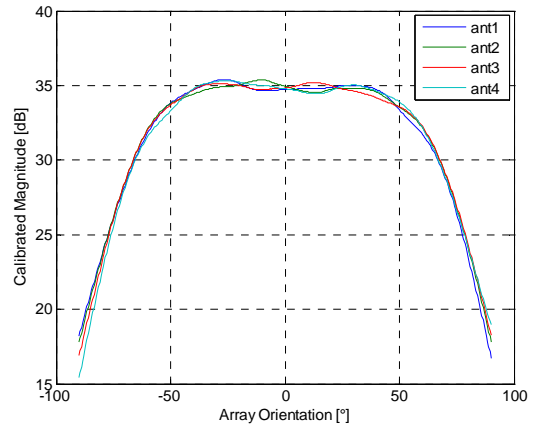


Figure 7(a). Calibrated ULA Tx beam patterns.

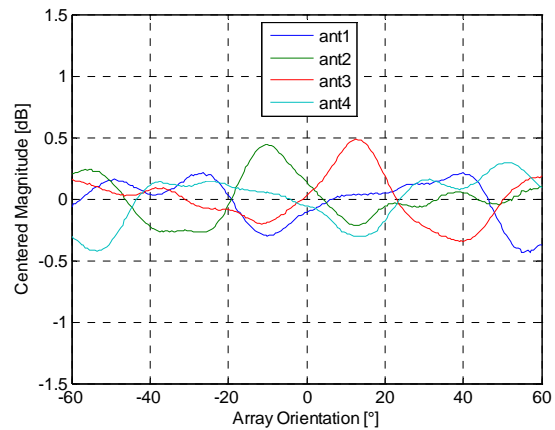


Figure 7(b). Calibrated ULA Tx beam patterns ripple.

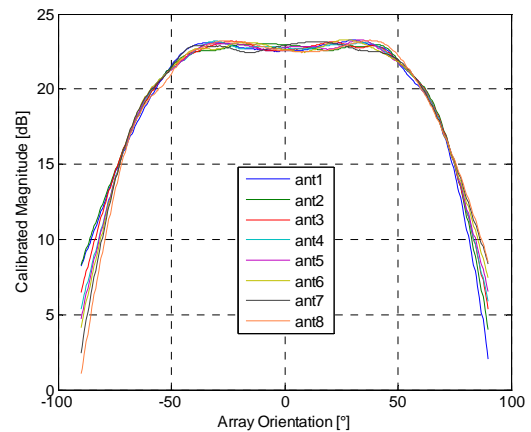


Figure 8(a). Calibrated ULA Rx beam patterns.

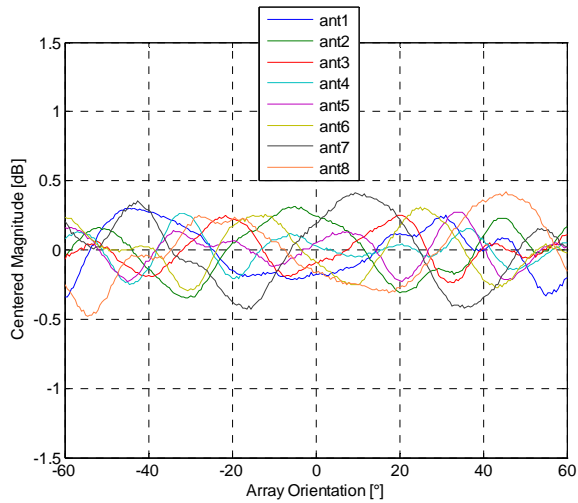


Figure 8(b). Calibrated ULA Rx beam patterns ripple.

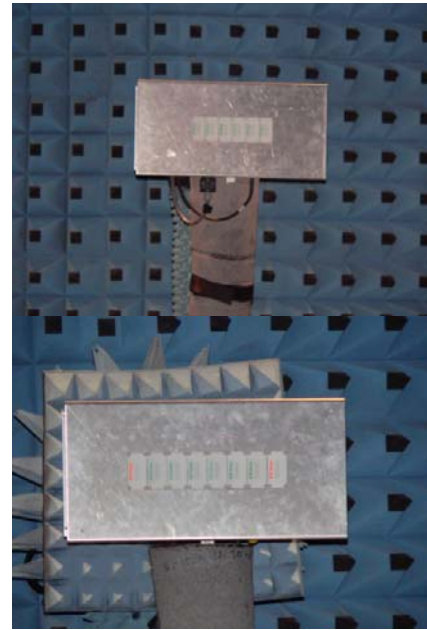


Figure 10. ULA Tx measurements configuration.

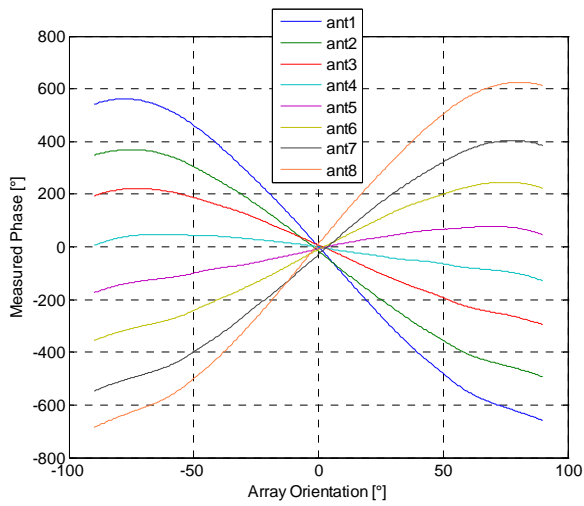


Figure 9(a). Measured ULA Rx phase.

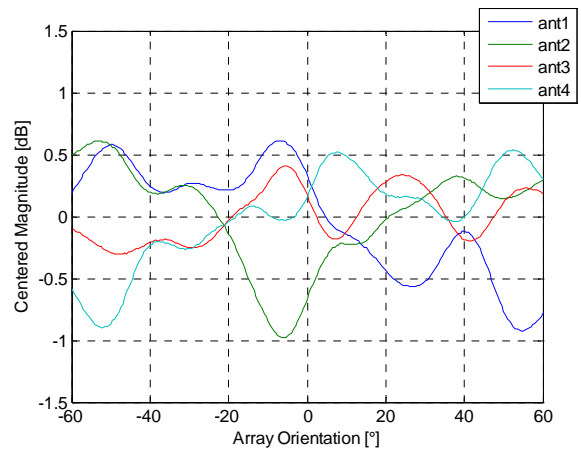


Figure 11(a). New ULA Tx beam patterns ripple.

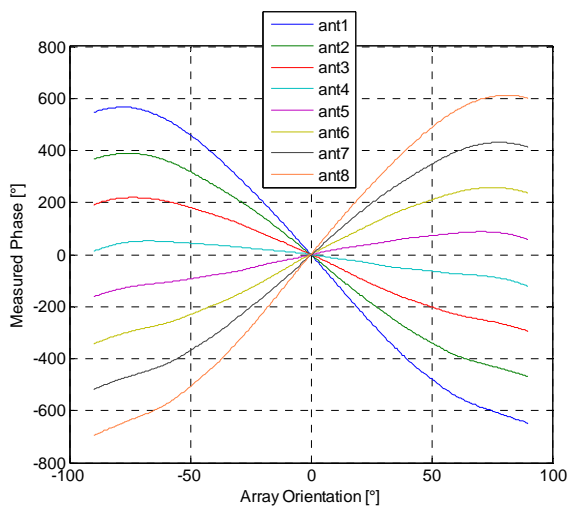


Figure 9(b). Calibrated ULA Rx phase.

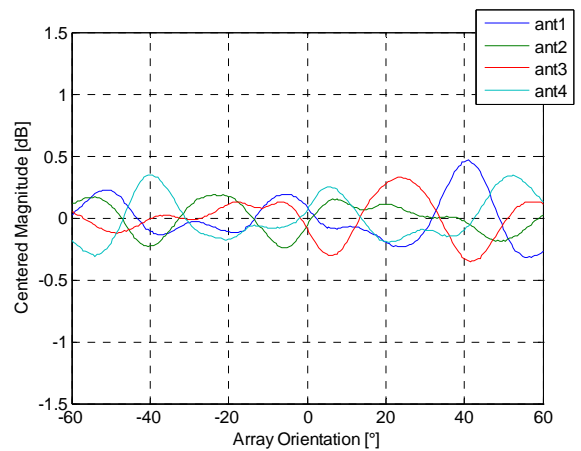


Figure 11(b). Calibrated ULA Tx beam patterns ripple.

VI. ESPRIT SIMULATIONS

In order to demonstrate the calibration need for high resolution channel sounding and to evaluate the performance of the antenna arrays, measured beam patterns were tested with ESPRIT algorithm [4]. We simulated 50 paths with their respective Directions of Arrivals (DOAs) and delays. Then, we estimated these parameters with ESPRIT algorithm.

In the first simulation, we used the measured beam patterns in anechoic chamber without calibration, and for the second one we used the calibrated beam patterns.

Fig. 12(a) shows the estimated parameters without calibration. We can observe the presence of parameters estimation errors. Fig. 12(b) shows the simulated and estimated parameters when we used the calibrated array. In this case, the estimation errors are significantly reduced.

The double directional propagation measurements performed with ULAs permits us to obtain the channel properties for a 120° sector. To obtain a full 360° azimuth, we have to rotate the planar arrays of 3x120° on the Tx and Rx side, and this rotation increases the measurements time. In this case, it is not possible to characterize the time variant behavior of the propagation

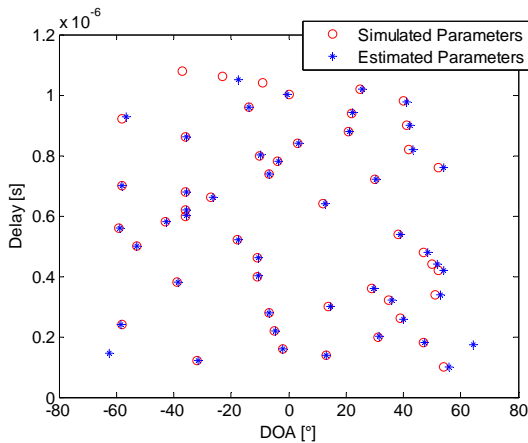


Figure 12(a). Simulation results without calibration.

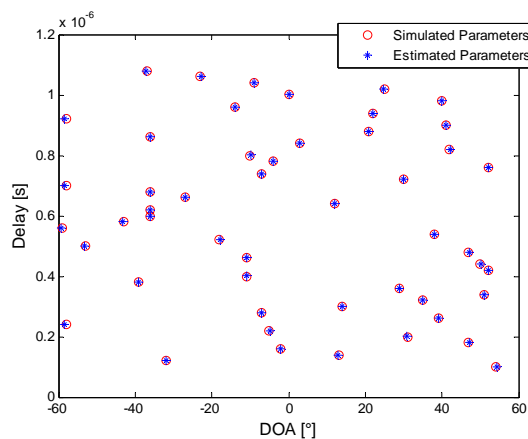


Figure 12(b). Simulation results with calibration.

channel. To solve this problem, new arrays architectures were studied, and we chose the UCA (Uniform Circular Array) architecture that enables us to measure full azimuthal double directional channel instantly at both Tx and Rx side without any rotation.

VII. NEW ARRAYS ARCHITECTURE

We developed a 4-active-element UCA transmitter, and we integrated also power amplifiers. Fig. 13 presents the 4-element UCA and Fig. 14 the measured beam patterns. The azimuthal beam width of each array element is larger than 90° which enables 360° characterization. At reception, a 16-element UCA array at 3.5 GHz was developed. As for the ULA receiver, we also integrated LNA. Fig. 15 (a) and (b) present the 16-element UCA at 3.5 GHz and the integrated components respectively. It is used to estimate DoA in the azimuth and elevation planes with ambiguity above and below the azimuthal plane of the array especially in indoor and outdoor-to-indoor environments. Fig. 16(a) shows the UCA 16-element measured horizontal cut of horizontal beam patterns at 3.5 GHz, which enables 360° azimuthal characterization, and Fig. 16(b) the UCA 16-element measured vertical cut of vertical beam patterns at 3.5 GHz, which offers 60° beam width for elevation measurement. With this new configuration, a full 360° azimuth measurement is instantly done.

To estimate propagation parameters with the UCA, we developed the high resolution algorithm SAGE (Space-Alternating Generalized Expectation Maximization) [15]. This algorithm is more efficient than ESPRIT for these antenna arrays architectures [16]. After the antenna arrays development, propagation measurement campaigns are currently in progress in different environments.

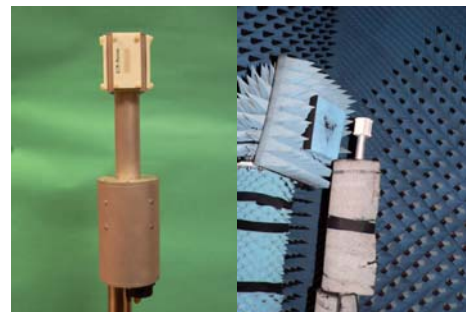


Figure 13. Four elements UCA Tx.

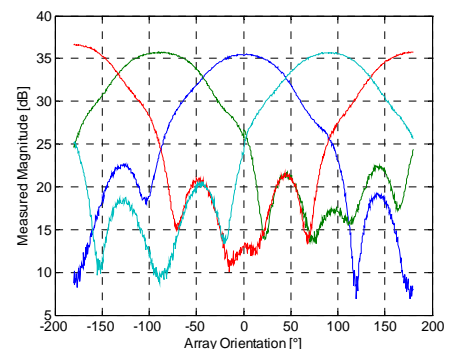


Figure 14. Measured beam patterns of 4 elements UCA Tx.

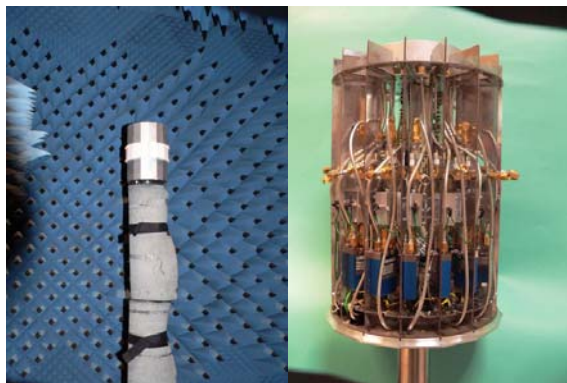


Figure 15 (a). 16 elements UCA Rx.

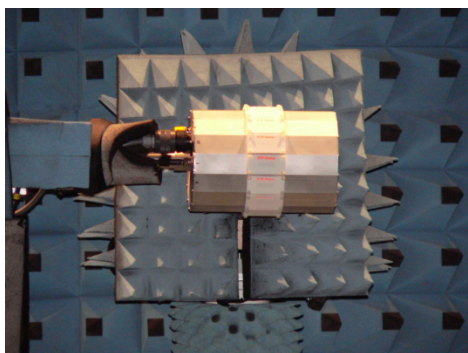


Figure 15 (b). Vertical patterns measurement configuration.

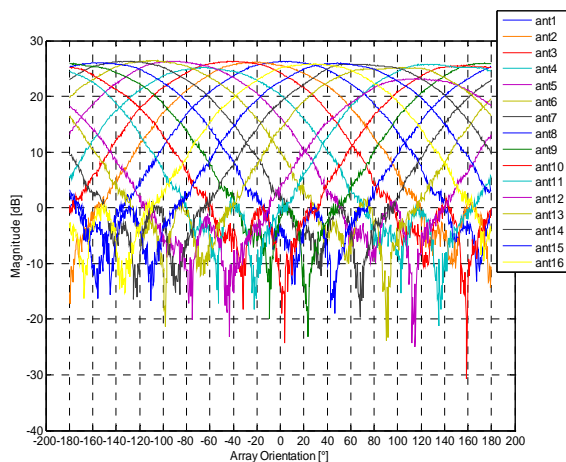


Figure 16 (a). UCA Rx measured horizontal beam patterns.

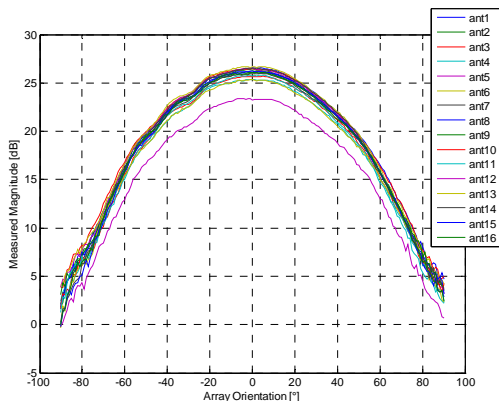


Figure 16 (b). UCA Rx measured vertical beam patterns.

CONCLUSIONS

In this paper, we presented a MIMO channel sounder at 3.5 GHz for double directional propagation radio channel characterization. The design and calibration of two linear antenna arrays for transmission and reception at 3.5 GHz is described. We presented beam patterns measurement results in anechoic chamber for the two arrays, and the effects of array imperfections on the measured beam patterns.

A calibration algorithm was applied on beam patterns measurements, and calibration results for the two arrays are presented. Simulation results with the high resolution ESPRIT algorithm showed the importance of the calibration procedure to obtain better multi-path parameters estimation.

New circular antenna arrays at transmission and reception are also presented. It allows a full azimuthal characterization of the directional channel.

In the perspectives of this work, propagation measurement campaigns, in various environments and with fixed configurations, are currently in progress. The statistical parameters obtained from these measurements are necessary to obtain realistic MIMO propagation channel models. These channel models are useful to define multiple engineering rules needed to design future MIMO wireless systems.

ACKNOWLEDGMENT

This work is part of the Techim@ges project of french “Media and Networks Cluster”. This project is financially supported in part by “Region Bretagne”.

REFERENCES

- [1] I. E. Telatar, “Capacity of multi-antenna Gaussian channels,” Tech. Rep. Atand T-Bell Labs, 1995.
- [2] G. J. Foschini, M.J. Gans, “On limits of wireless communications in a fading environment when using multiple antennas,” *Wireless Personal Communications*, Vol. 6, No. 3, pp. 311-335, Mar. 1998.
- [3] R. Cosquer, “Conception d’un sondeur de canal MIMO. Caractérisation du canal de propagation d’un point de vue directionnel et doublement directionnel,” Ph.D. Thesis in electronics, INSA Rennes, Oct. 2004.
- [4] M. Haardt, “Efficient one-, two and multidimensional High Resolution Array Signal Processing,” Ph.D. Thesis, TU-Munich, Germany, 1996.
- [5] M. Tschudin et al., “Comparison unitary ESPRIT and SAGE for 3-d channel sounding,” *In Proc. IEEE VTC*, pp. 1324-1329, May 1999.
- [6] H. Farhat, G. El Zein, “Antenna arrays design and calibration for high resolution MIMO channel sounding at 3.5 GHz,” *In Proc. IEEE VTC Fall 2007*, pp. 936-940, Baltimore, USA, Sept. 2007.
- [7] M. Steinbauer, A. F. Molisch, E. Bonek, “The double directional radio propagation channel,” *IEEE Antennas and propagation Magazine*, Vol. 43, pp. 51-63, 2001.
- [8] P. Almers, E. Bonek, A. Burr et al., “Survey of Channel and Radio Propagation Models for Wireless MIMO Systems,” in *EURASIP Journal on Wireless Communications and Networking*, Vol. 2007, Article ID 19070, 19 pages, 2007.

- [9] <http://www.elektrobit.com>
- [10] <http://www.channelsounder.de/mimoextension.html>
- [11] V. Kolmonen, J. Kivinen, L. Vuokko, P. Vainikainen, "5.3-GHz MIMO Radio Channel Sounder," *IEEE Trans. On Instrum. Measur.*, Vol. 55, No. 4, pp. 1263-1269, Aug. 2006.
- [12] P. Lehne et al., "Calibration of mobile radio channel sounders," *COST 259*, TD-98, Duisburg, Germany, Sept. 1998.
- [13] K. Pensek and J. A. Nossek, "Uplink and downlink calibration of an antenna array in mobile communication system," *COST 259*, TD 97(55), Feb. 1997.
- [14] G. Sommerkorn, et al., "Reduction of DoA estimations errors caused by antenna array imperfections," *In Proc. 29th European Microwave Conference*, Munich, Germany, Vol. 2, pp. 287-290, 1999.
- [15] B. H. Fleury et al., "Channel parameter estimation in mobile radio environments using the SAGE algorithm," *IEEE JSAC*, Vol. 17, No. 3, pp. 434-449, Mar. 1999.
- [16] C. M. Tan et al., "On the application of circular arrays in direction finding, Part I: Investigation into the estimation algorithms," Companion paper in 1st Annual COST 273 Workshop, Espoo, Finland, May 2002.

Hanna Farhat received his B.S. in Telecommunications and Networking from the Lebanese University saïda, Lebanon, in 2001, and the M.S. degree in electronics from INSA de Rennes, France in 2004.

He is now pursuing his PhD thesis in electronics at IETR. His research interests includes MIMO channel sounding and propagation channel parameters estimation.

Guy Grunfelder is a CNRS engineer. He worked with LCST – INSA de Rennes since 1988 to 2001. And since 2002, he works with IETR.

His research activities include system design and implementation. He also works on antenna conception and realization, and is involded in many research projects.

Alvaro Carcelen received master's degree in Telecommunications engineering from the Polytechnic University of Cartagena (UPCT), Spain, in 2006. His final degree project was developed in 2005-2006 at IETR.

He joined IETR since May 2007 as a research engineer. He is working on the development of a high-resolution method for the estimation of the channel characteristics, and assisting in the MIMO measurement campaigns.

Ghaïb El Zein received the Ph.D. and Habilitation a Diriger des Recherches (HDR) degrees in Telecommunications—Signal processing and Electronics from Rennes 1 University, France, in 1988 and 1998, respectively.

From 1985 to 1987, he was a Lecturer, and from 1990 to 1999, an Associate Professor, in the Department of Electronics and Communications Systems Engineering, INSA de Rennes,

where he is currently a Professor. His teaching and research interests mainly concern the study of radio wave propagation phenomena and the evaluation of their effects on communication systems performance. Since 2001, he has been the Assistant Director of the IETR. He is a member of CNFRS-URSI.